EVALUATION OF LOW-FREQUENCY BOTTOM BACKSCATTERING STRENGTH VS GRAZING ANGLE BY MEANS OF MULTIPLE BEAMFORMING

D. Marandino and T.G. Goldsberry
SACLANT ASW Research Centre
Viale San Bartolomeo 400
I-19026 La Spezia, Italy

ABSTRACT

Bottom backscattering strength was measured in deep water as a function of grazing angle in the Balearic Abyssal Plain of the Mediterranean. The measurements were made with a towed, narrowband low-frequency omnidirectional source and a towed, horizontal linear array. The method takes advantage of the multiple beamforming capability of the receiving array and processor to accurately discriminate returns at given grazing angles from interfering returns. Approximations for the evaluation of the backscattering area are described and discussed. The results are presented and compared with previously reported measurements. At the higher grazing angles, specular reflection from normal incidence dominates the returns. However at medium and small grazing angles data have a large plateau region, with small variations. A Lambert's rule relationship, with a coefficient of -33 dB, can approximate results for grazing angles as low as about 20°.

INTRODUCTION

Low-frequency bottom backscattering strength values have been previously measured and reported by several authors [1 to 5]. These results refer to experiments with broad-band sources (explosives) and omnidirectional receivers. However the data presented herein were collected using narrowband sources and directional receivers. By taking advantage, on reception, of the directional properties of a towed linear array, it was possible to accurately discriminate returns at various grazing angles. Indeed, it is well known that beams formed by a linear array have conical symmetry around the array's axis. This property was exploited to discriminate returns in the vertical plane and to estimate arrivals from progressively longer times and thus smaller grazing angles.

Measurements were made in a deep water area in the Balearic Abyssal Plain. While the results are pertinent only to a similar environment the evaluation criteria can be generally applied to horizontal towed arrays.

The next section provides a description of the experiment and is followed by a discussion on the measurement criteria that emphasizes the evaluation of the backscattering area. Finally, the results are presented and discussed.

1 DESCRIPTION OF THE EXPERIMENT

The experiment was conducted in an area of the Balearic Abyssal Plain which is typical of Mediterranean-type abyssal plains. The water depth at the site is 2800 m. Cores, 6 m long that were previously collected in the same area, show layers of sand interspersed with thin layers of clayey and silty deposits. An isothermal water column was present, giving rise to typical Mediterranean winter propagation conditions characterized by a totally upward refracting profile. Wind speed was less than 7 kn and sea state was 1 to 2, with a moderate swell.

The experimental set-up for the collection of monostatic reverberation used the SACLANTCEN R/V Maria Paolina to tow a sound source and a linear array receiver at constant speed, course and depth. During the run, the source generated pulses at regular intervals, and the bottom echoes were received by the towed linear array and subsequently processed on board. Both the source and array depth were 100 m.

Figure 1 shows a simplified block diagram of the data acquisition and processing system. The array has 32 hydrophones with half wavelength spacing. Hamming shading is applied to the hydrophone data. The filtered and digitized returns are beamformed via a time-domain, programmable multiple beamformer, and subsequently match-filtered in the array processor. Figure 2 depicts the beamformer file that was used during the experiment and indicates both a plan and side view of the beam-pointing directions, as determined by conical symmetry and assuming a constant sound speed profile.

The transmitted waveform was a linear frequency modulated (LFM) pulse with a one second duration and 10 Hz swept bandwidth at a centre frequency of 365 Hz. The received signals were processed through a quadrature replica correlator with Hanning shading; the final equivalent slant range resolution is approximately 120 m.

2 BOTTOM SCATTERING STRENGTH EVALUATION METHOD

2.1 The Data Base

Returns from a number of pings were ensemble-averaged to determine a mean reverberation envelope. Reverberation at initial ranges is dominated by bottom backscattering that affects returns in two distinct ways:

- The first is referred to as the "fathometer effect", and is caused by the energy that is radiated by the omnidirectional source in the vertical direction and that propagates vertically in the water column, repetitively bouncing off the bottom and the surface. This is evidenced in the processed beam output time series as a sequence of peaks of the received power, which are regularly spaced at a distance equal to twice the water depth.

- The second effect is the progressive decay of the received power which is caused by backscattering from the bottom at progressively longer ranges, and thus smaller grazing angles.

Both effects can be seen in Fig. 3 where the ping-to-ping (ensemble) average of the returns received at the broadside beam over a limited set of ranges is shown on a logarithmic scale in an A-scan format. Also shown is the measured ambient noise level in the processed band (noise floor). The lower half shows the standard deviation of the averaging procedure of

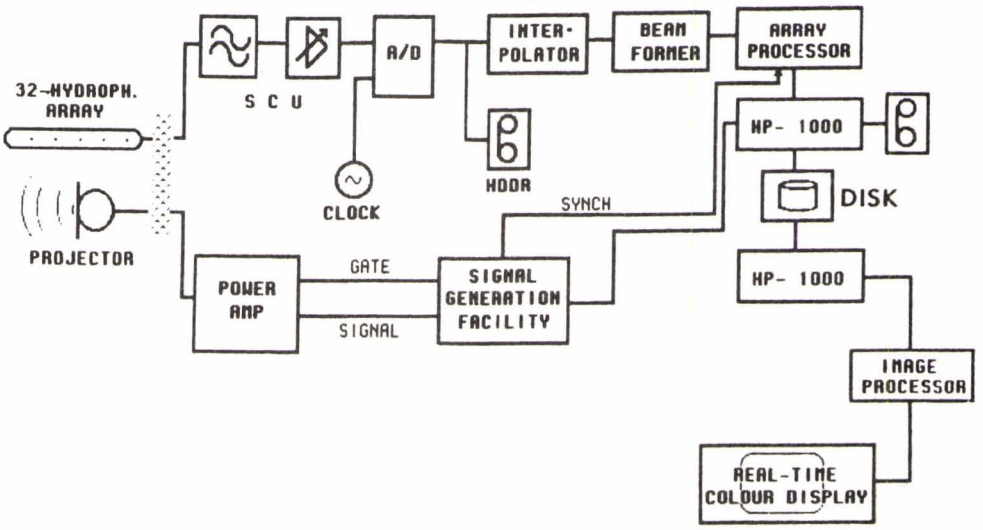

Fig. 1 Block diagram of SACLANT's data acquisition and processing system for reverberation measurements.

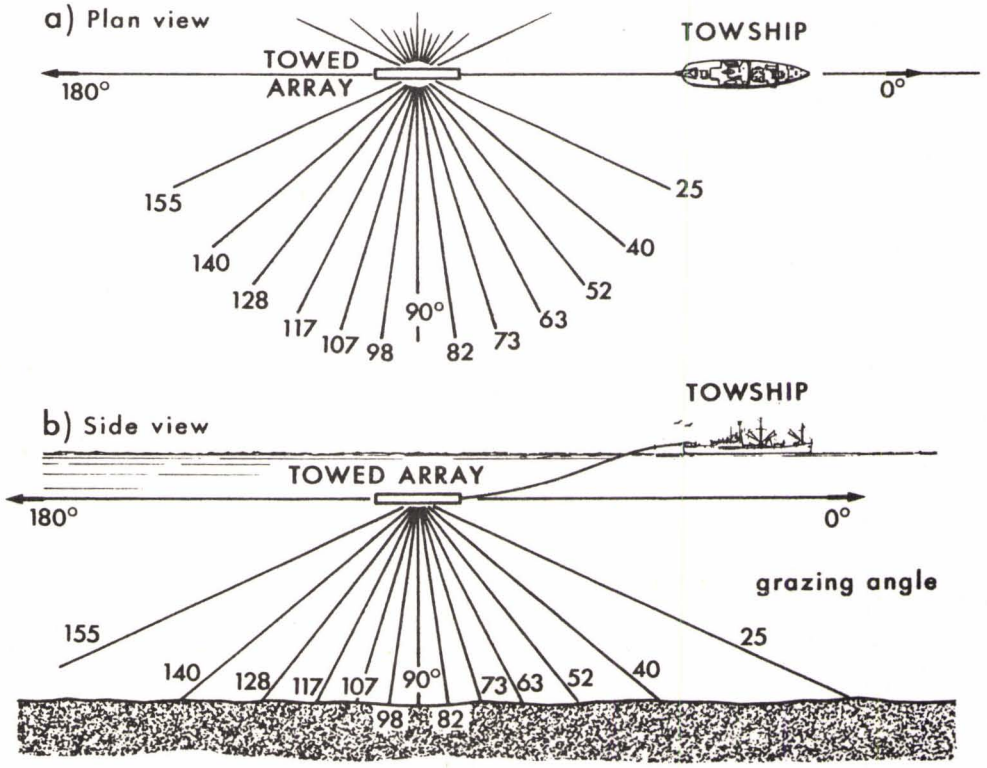

Fig. 2 Beam geometry of low frequency bottom backscattering experiment.

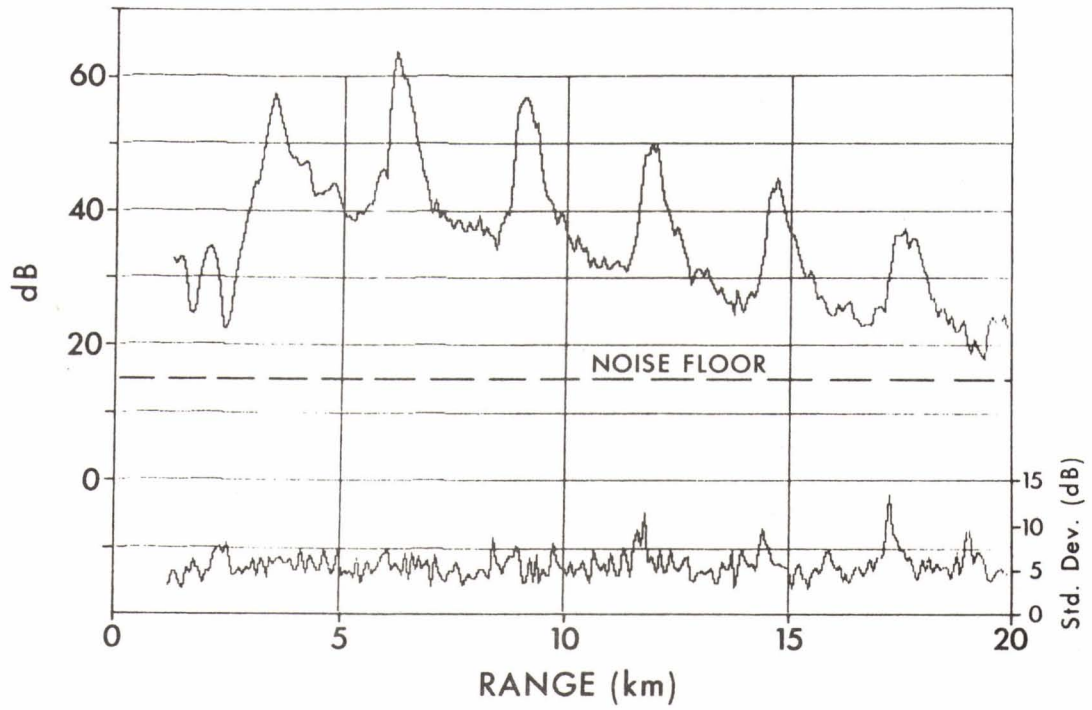

Fig.3 Average of reverberation returns received at the 90° beam, ambient noise floor, and standard deviation. (water depth: 2800 m; centre frequency: 365 Hz).

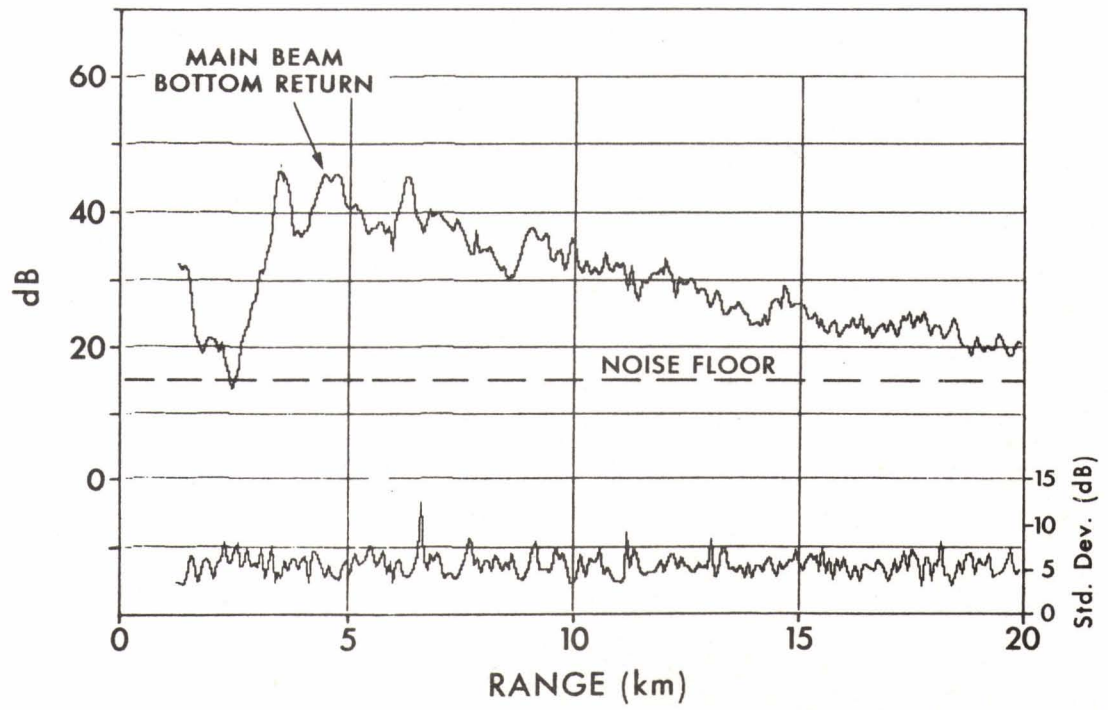

Fig. 4 Average of reverberation returns at the 38° from broaside beam, ambient noise floor, and standard deviation. (water depth: 2800 m; centre frequency: 365 Hz).

the figure which has a mean value of 5.5 dB, as expected from the averaging of Rayleigh distributed log normalized data. The fathometer peaks and the regular decay of bottom reverberation vs range are evident. However, broadside beam data cannot be used to accurately determine bottom backscattering strength because of the high sidelobes associated with the fathometer returns. To overcome that, the data from the off-broadside beams have been used. In this case, the fathometer effect is attenuated because vertically propagating energy is picked up through the angular sidelobes of the various beam patterns. Also, the beam power time series shows a local maximum corresponding to the onset of the bottom returns at the grazing angle related to the main beam pointing direction. This correspondence confirms the hypothesis of the predominance of bottom reverberation.

This is illustrated in Fig. 4 which show the time series associated with the beam pointing at 38° from broadside, which corresponds to a 52° grazing angle. An arrow marks the main beam bottom return. The advantages of evaluating backscattering strength in this manner are that: a) a (local) maximum of the signal-to-noise ratio is used; b) the influence of the fathometer effect can be considered negligible; c) the propagation loss can easily be estimated by assuming spherical spreading.

Bottom backscattering strength vs grazing angles can then be determined by direct application of the sonar equation, using the power output time series of the various beams.

2.2 Evaluation of the Backscattering Area

In order to determine scattering strength by means of the sonar equation, an estimate of the backscattering area (A_b) must be obtained. The evaluation of A_b is determined by three factors: propagation mechanism, the characteristics of the waveform and the beam shape at reception.

Figure 5 provides a plan and side view of the geometry of the experiment which is applicable to the evaluation of A_b and defines the pertinent axes and parameters. The y-axis is orientated along the array axis direction. In the figure,

A_{bM} is backscattering area at medium to small grazing angles

A_{bH} is backscattering area at high grazing angles

d_w is water depth

h is water depth less source depth

γ is the grazing angle (angle between bottom and propagation path)

γ_{eq} is the "equivalent" grazing angle, at small grazing angles

d_r is the annular width related to the signal range resolution

d_b is the annular width related to the mainbeam intersection and

d_{cr} is the "cross-range" dimension of A_b.

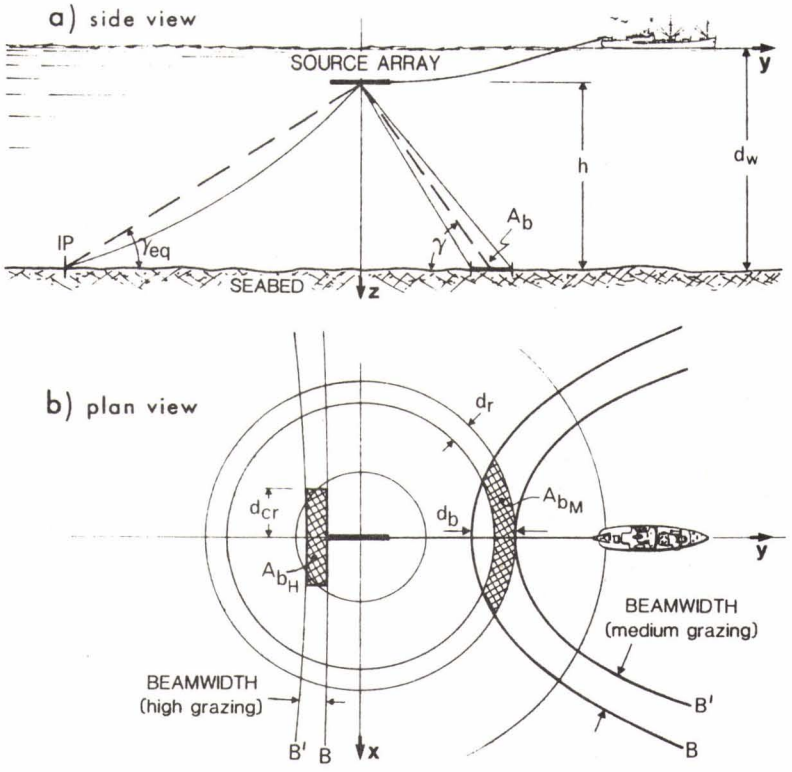

Fig. 5 Geometry for the backscattering area.

The energy radiated by the source propagates spherically and intersects the (flat) bottom along circles, whereas the various beams, which define cones around the array axis, intersect the bottom along hyperbolic curves B and B' in Fig. 5. However, such representation is only applicable to high and medium grazing angles (> 20°) where ray bending caused by the true sound speed profile are negligible. In this case the grazing angle is also equal to the complementary angle of the ray at the source/receiver. For smaller grazing angles, say below 20°, it has been assumed that the geometry remains approximately valid, provided that the actual grazing angle is replaced by an "equivalent" angle obtained by the straight-line approximation to the actual intercept point (IP in the figure) as determined by the actual sound speed profile. For this experiment, the ray at 13.86° at the source grazed the bottom at 0° with an equivalent grazing angle of 6.93° and slant range of 22370 m.

For an omnidirectional receiver, power comes from a circular annulus with a width (d_r) expressed by:

$$d_r = d_s \,/\, \cos(\gamma) \qquad (1)$$

where d_s = slant-range signal resolution (here, 120 m).

Since the receiver is directional, only that part of the annulus which is included in the mainbeam contributes to backscattering, under the assumption that contributions from the beam's sidelobes are negligible. The intersection of the mainbeam with the bottom (hyperbolic curves B and B' in Fig. 5) is expressed by:

$$y_i^2 = \frac{x^2 + h^2}{2} \quad ; \; i = 1, 2 \qquad (2)$$

where γ_1 and γ_2 are the grazing angles corresponding to the 3 dB beamwidth.

This area has a minimum radial width, d_b, along the trace of the array axis on the bottom, expressed by

$$d_b = h * b_w(90°) / [\sin(\gamma)]^3 \qquad (3)$$

where $b_w(90°)$ = array beamwidth at broadside, with the assumption that the beamwidth for any beam pointing direction is given by

$$b_w(\gamma) = b_w(90°) / \sin(\gamma).$$

The backscattering area can then be estimated through the rectangular approximation:

$$A_b = D_r * D_{cr} \qquad (4)$$

where D_r is the radial dimension, and

D_{cr} is the cross-range dimension.

Two cases may thus be distinguished:

- $d_r > d_b$. This is valid at high grazing angles (A_{bH} in Fig. 5). In this case the width of the transmission annulus is larger than the width of the hyperbolic annulus generated by the mainbeam intersection; therefore, in Eq. 4 it is:

$$D_r = d_b \qquad (5)$$

- and, for the cross-range dimension, simple geometrical considerations on returns included between R and $R+d_s$, where R is the slant range in the mainbeam give:

$$D_{cr} = 2\, d_s \sqrt{\left(1 + \frac{2h}{d_s \sin\gamma}\right)} \qquad (6)$$

- $d_r < d_b$. This is valid at medium to small grazing angles. The backscattering area (A_{bM} in Fig. 5) is that part of the circular annulus that is delimited by the intersection with the beam hyperbola. For a given range, the area can then be expressed by the rectangular approximation (4), where the radial dimension is

$$D_r = d_r\ , \qquad (7)$$

and the cross-range dimension D_{cr} is the arc of circle generated by the intersection of the lowermost hyperbola and the circle related to that range. Then:

$$D_{cr} = \frac{2h}{\tan\gamma_R} \cdot \arcsin \sqrt{\frac{\tan^2\gamma_L - \tan^2\gamma_R}{1 + \tan^2\gamma_L}}$$

where γ_L = higher grazing angle, which corresponds to the 3 dB beamwidth boundary

γ_R = grazing angle corresponding to the given range.

At small grazing angles, however, ray bending increases the distance at which the rays intercept the bottom and the beam intersections with the seabed are not expressed as hyperbolas. However the evaluation of A_b is still based on formulas (7) and (8), in which equivalent grazing angles that correspond to the linear approximation to the actual rays are used.

The relationship between the actual and the equivalent grazing angle can easily be established since the experiment was carried out in isothermal water and thus with a constant velocity gradient. In this case the rays are arcs of circles whose centers lay at a fixed distance

$$R_o = C_{REF} / \zeta \qquad (9)$$

where

C_{REF} is the reference sound velocity (1500 m/s), and

ζ is the velocity gradient (0.017 s^{-1})

It is then:

$$\cos \gamma = (1 + \frac{h}{R_o}) \cos \gamma_{RAY} \qquad (10)$$

and

$$\gamma_{eq} = \frac{1}{2} (\gamma_{RAY} + \gamma) \qquad (11)$$

where

γ is the angle of the grazing ray

γ_{RAY} is the angle of the (monostatic) ray at the source/array and

γ_{eq} is the equivalent grazing angle.

The approximations used in the evaluation of A_b at small grazing angles can be considered satisfactory because d_r is much smaller than the other dimensions.

The behaviour of the bottom backscattering area for beams off broadside, as a function of the true grazing angle, is indicated in Fig. 6 along with the two-way propagation loss at the pertinent ranges. A_b is expressed in dB relative to one square meter and is evaluated with the parameter values applicable to the experiment.

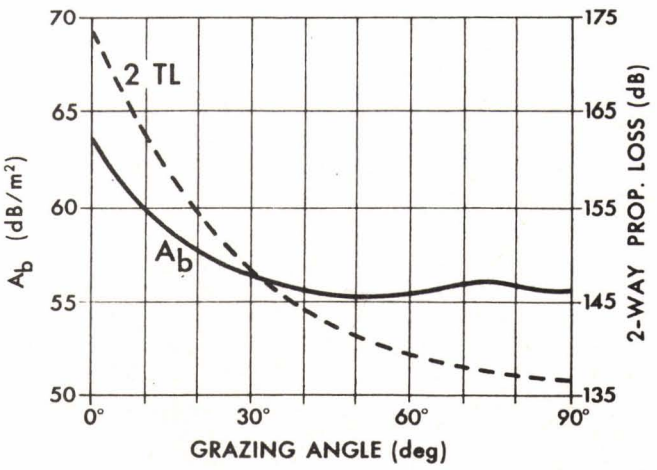

Fig. 6
Bottom backscattering area and two-way propagation loss as a function of the true grazing angle.

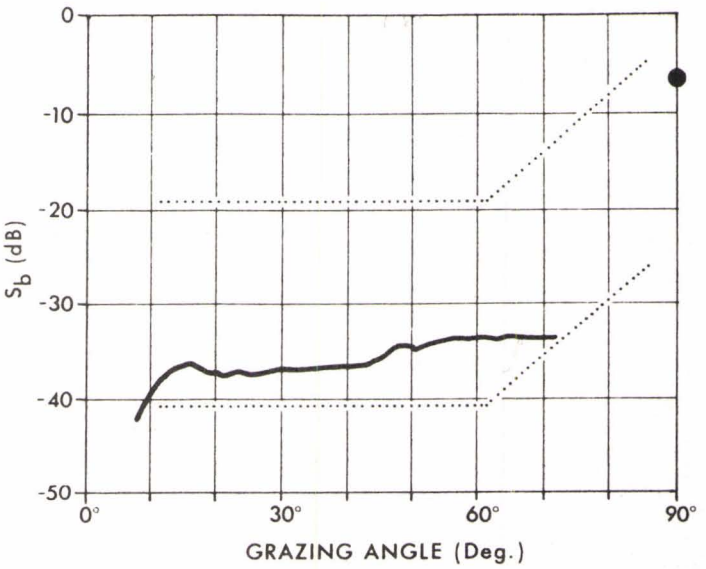

Fig. 7
Backscattering strength coefficient s_b, versus grazing angle, at a centre frequency of 365 Hz. The dotted lines show the limits of reported values for low frequency bottom backscattering strength.

3 RESULTS AND CONCLUSIONS

By applying the sonar equation [6] and using the appropriate curves for the backscattering area and the propagation loss, a point estimation of the backscattering strength coefficient versus grazing angles is obtained (see solid line in Fig. 7).

Two cases must be distinguished:

- At high grazing angles, because of the signal slant-range resolution returns from 73° to 90° cannot be separated and are merged into the fathometer peak and sidelobes. Nevertheless, the fathometer peak itself can be regarded as high grazing angle backscatter. Therefore, an estimation of S_b at near incidence can be obtained by measuring the power at the peak of the fathometer return. However, since the first-bounce fathometer return saturates the hydrophones, it is impossible to determine S_b reliably. Instead the second-bounce fathometer return was used with the addition of the estimated bottom loss incurred at the first bounce (6 dB). The applicable backscattering area here is that of the broadside beam at 90°. The result is given in Fig. 7 by the value at the 90° grazing angle.

- The evaluation of S_b for medium to small grazing angles is outlined in Sect. 2.2. Both rear and forward beam pointing directions were used; however forward beams have a higher noise level due to the towship contributions and are not suitable for estimates at small grazing angles. The estimate is quite accurate for angles above 30° because the backscattering area has small variations and, more importantly, because the measurements are made before the onset of the second fathometer return and are thereby free of multiple bounce scattering. At smaller grazing angles, the estimate of S_b becomes more difficult because the output ratio of signal-to-ambient noise is lower, small variations of the array tilt cause large variations of the intercept area and contributions from multiple-bounce scattering are more likely. However measurements can still be made and an approximate, upper bound for S_b can be obtained for these smaller grazing angles.

The overall behaviour of the bottom backscattering strength indicated in Fig. 7 shows that S_b has high values in that region where backscattering is dominated by specular reflection. The range of angles of high backscattering is determined by the system geometry and the type of

waveform such that the coherent (specular) component dominates incoherent (diffuse) scattering.

For decreasing angles, S_b quickly decays by about 30 dB. Then, for medium and small grazing angles, it has a plateau region where the variations are small. Values of -33 to -37 dB are measured for medium angles (60° to 30°) and of -40 to -42 dB for smaller angles (around 10°).

A comparison with Lambert's rule for diffuse backscattering shows that a value of -33 dB for the Lambert coefficient is reasonable for medium grazing angles. The limits of reported data for low-frequency bottom backscattering strength range from -20 to -40 dB, and are shown in Fig. 7 by the dotted lines (see, for instance, Ref. 6, page 246). These include results at various frequencies and for different types of bottom. As can be seen, the range of previously reported data spans the present measurements, although similar types of seafloor are usually assumed to have slightly higher S_b values.

In conclusion, a method has been presented to evaluate low frequency bottom backscattering strength which takes advantage of the multiple beamforming capability of a towed linear array. The intrinsic system directivity confines backscattering to small, homogeneous seafloor patches and suppresses interference from other directions.

REFERENCES

1. K.V. Mackenzie, Long range shallow-water bottom reverberation, J. Acoust. Soc. Amer. 34: 62-66 (1962).
2. R.J. Urick and D.S. Saling, Backscattering of explosive sound from the deep-sea bed, J. Acoust. Soc. Amer. 34: 1721-1724 (1962).
3. A.W. Burstein and J.J. Keane, Backscattering of explosive sound from ocean bottoms, J. Acoust. Soc. Amer. 36: 1596-1597 (1964).
4. P.B. Schmidt, Monostatic and bistatic backscattering measurements from the deep ocean bottom, J. Acoust. Soc. Amer. 50: 327-331 (1971).
5. H.M. Merklinger, Bottom reverberation measured with explosive charges fired deep in the ocean, J. Acoust. Soc. Amer. 44: 508-513 (1968).
6. R.J. Urick, Principles of Underwater Sound, 2nd ed. New York, NY, McGraw-Hill (1975).